Journal of Colloid and Interface Science 440 (2015) 229–235

Contents lists available at ScienceDirect

Journal of Colloid and Interface Science

www.elsevier.com/locate/jcis

Hierarchical opal grating films prepared by slide coating of colloidal dispersions in binary liquid media

Wonmok Lee [a,*], Seulgi Kim [a], Seulki Kim [a], Jin-Ho Kim [b], Hyunjung Lee [c,*]

[a] Department of Chemistry, Sejong University, 98 Gunja-dong, Gwngjin-gu, Seoul 143-747, Republic of Korea
[b] Korea Institute of Ceramic Engineering and Technology, Icheon, Gyeonggi 467-843, Republic of Korea
[c] School of Advanced Materials Engineering, Kookmin University, 861-1 Jeongneung-dong, Seoul 136-702, Republic of Korea

ARTICLE INFO

Article history:
Received 6 July 2014
Accepted 12 October 2014
Available online 11 November 2014

Keywords:
Opal
Alcoholic media
Slide coating
Groove pattern
Grating

ABSTRACT

There are active researches on well ordered opal films due to their possible applications to various photonic devices. A recently developed slide coating method is capable of rapid fabrication of large area opal films from aqueous colloidal dispersion. In the current study, the slide coating of polystyrene colloidal dispersions in water/i-propanol (IPA) binary media is investigated. Under high IPA content in a dispersing medium, resulting opal film showed a deterioration of long range order, as well as a decreased film thickness due to dilution effect. From the binary liquid, the dried opal films exhibited the unprecedented topological groove patterns with varying periodic distances as a function of alcohol contents in the media. The groove patterns were consisted of the hierarchical structures of the terraced opal layers with periodic thickness variations. The origin of the groove patterns was attributed to a shear-induced periodic instability of colloidal concentration within a thin channel during the coating process which was directly converted to a groove patterns in a resulting opal film due to rapid evaporation of liquid. The groove periods of opal films were in the range of 50–500 μm, and the thickness differences between peak and valley of the groove were significantly large enough to be optically distinguishable, such that the coated films can be utilized as the optical grating film to disperse infra-red light. Utilizing a lowered hydrophilicity of water/IPA dispersant, an opal film could be successfully coated on a flexible Mylar film without significant dewetting problem.

1. Introduction

Three-dimensional (3D) photonic crystals of submicrometer wavelength range have gathered much attention due to its potential applications to photonic devices such as microlasers [1,2] optical waveguides, and chemical sensors [3,4]. Among various fabrication strategies for the 3D photonic crystal scaffolds, artificial opal films are frequently utilized as they can be readily obtained from self-assembly process of monodisperse microspheres (diameter = 0.1–1 μm) in the liquid media. If the surface of microsphere is polar enough to be dispersed in water, strong capillary forces between microspheres induce the ordered arrangements of the particles into an opal film upon water evaporation. The resulting opal film exhibits shiny reflective color, so called structural color depending on the particle size due to Bragg diffraction of visible light from the periodic [1 1 1] facets of face centered cubic (fcc) crystalline structure within the opal film. Various fabrication methods for capillary-induced opal films have been developed such as dip-coating [5–8], direct-coating [9,10], and capillary method [11–13]. Dip-coating method has been commonly adopted since it provides high quality opal films, while the process is too slow and consumes too much colloidal dispersion. In the capillary methods, the colloidal dispersion is filled within the capillary channel and subsequently dried. This method is much faster than dip-coating, and the resulting opal film conforms to the shape of capillary channel. Recently, direct coating method has been reported to be capable of rapid fabrication of large area opal films. P. Jiang and coworkers utilized Doctor Blade™ to spread the colloidal suspension which subsequently dried to form well-ordered opal film with area of 10 cm^2 within 30 min [14]. Lee et al. have also demonstrated a slide coating method in which a large area polymeric opal films were fabricated less than an hour by supplying hot air to the colloidal suspension between the slide glasses to accelerate water drying. This method was simple yet effective way to produce polymer opal films [15] or binary films of polymer opal and TiO_2 nanoparticles filling the interstices [16]. In slide coating

* Corresponding authors. Fax: +82 2 3408 4317.
E-mail addresses: wonmoklee@sejong.ac.kr (W. Lee), hyunjung@kookmin.ac.kr (H. Lee).

http://dx.doi.org/10.1016/j.jcis.2014.10.051
0021-9797/

method, colloidal dispersions have been prepared in water to maximize the capillary force. However, it is desirable to test various polar solvents or their mixtures as dispersing agent of the colloidal particles to extend the applicability of the coating method.

In this study, the polystyrene (PS) colloidal dispersions in water/alcohol binary mixture are slide-coated on glass substrate by controlling the alcohol content. Morphological changes and surface structures of the resulting opal films accompanied in the course of film coating process are rigorously characterized [15].

2. Experimental

2.1. Synthesis of PS colloids

Spherical PS colloidal particles with two different particle sizes were synthesized by a typical emulsion polymerization method using potassium persulfate (PPS, Aldrich) and sodium dodecylsulfate (SDS, Aldrich) as a radical initiator and a surfactant respectively. Synthetic details are almost the same as described in the previous report [17]. Owing to the sulfate groups of PPS, the surface of the resulting colloidal particles is negatively charged in water, and therefore a stable aqueous colloidal dispersion is obtained. The synthesized PS particles were dialyzed using a semipermeable cellulose membrane (MWCO 12,000–14,000, MFPI) within deionized water for 2 weeks for purification, and the final aqueous dispersions contained 10 wt% solid contents. Two PS colloidal systems synthesized in this study were PS240 and PS 280 indicating that the average diameters of the PS colloids are characterized to be 240 nm and 280 nm respectively by using scanning electron microscopy (SEM, S-4700, HITACHI).

2.2. Slide coating of colloidal dispersions

As shown in Fig. 1(a), the apparatus for slide coating has a very simple configuration composed of top and bottom slide glasses, Teflon™ tape spacers (thickness ~ 200 μm) attached on each side of a bottom slide which is slowly pulled out by a syringe pump (KD scientific) at the controlled speeds. An aqueous PS dispersion was mixed with 2-propanol (IPA, 99%, Aldrich) at various mixing ratios, and then was infiltrated to a thin space between two slide glasses. As the bottom substrate moves out at a programmed speed, the colloidal self-assembly takes places at the drying front aided by hot air blown onto the drying film surface. The coated opal films were analyzed by SEM and a digital single lens reflex (DSLR) camera (DSLR-A550, SONY). The reflectance of a film was measured using a fiber optic UV–Vis spectrometer (AvaSpec, Avantes) connected to the reflected light microscopy (L2003A, Bimeince) through an objective lens (20×/0.30NA) as shown in Fig. 1(b). In each measurement, the raw data of reflected signal from the sample were referenced by a silver mirror (Edmund optics).

3. Results and discussion

The PS particles were initially dispersed in water, and subsequent addition of alcohol changed the physical property and the concentration of the dispersion. For both PS240 and PS280, the five colloidal dispersions in water/IPA with 25%, 40%, 50%, 60%, and 75% of IPA volume ratios were prepared, which respectively contained 7.5%, 6%, 5%, 4%, and 2.5% of PS particles. Those dispersions were slide-coated on clean glass slides at an optimized coating speed of 1 mm/min which provided the best film quality compared to other coating speeds [18]. (see Fig. S1 in supplementary material for the films prepared at various speeds.) Shown in Fig. 2(a)–(e) is the photographs of the opal films from the five dispersions of PS280 in order of increasing IPA content exhibiting red reflective colors owing to the Bragg diffraction of light from fcc (1 1 1) planes of opals. (The five sequential films from PS240 are shown in Fig. S2.) The color becomes less intense as the IPA content increases in the dispersion due to weakening in long-range order of colloidal crystals. The surface morphologies of the opal films are shown in Fig. 2(f)–(j) which reveal gradual deterioration of the hexagonal packing and increasing tendency of the defect densities with increased IPA content. For Fig. 2(f)–(j), the loosened hexagonal packing and occurrence of the linear dislocations such as the breakage of hexagonal lattice are dominant among which Fig. 2(j) (a film from 75% IPA) is most serious. The cross-sections of the films shown in Fig. 2(k)–(o) also present the changes in opal film qualities, along with the thickness decreases due to the dilution effect. Relatively random orientation of the colloidal film from a 75% IPA dispersion resulted in a weakening of a red reflective color. The quality of the opal film represented by the reflective color can be more rigorously traced by reflectance measurement of light under normal incidence, in which peak reflectance (λ_{peak}) has a linear relationship with particle size (d) by a modified Bragg equation as shown in Eq. (1) [15]:

$$\lambda_{peak} \sim 1.633 \cdot d\left(f_{PS} \cdot n_{PS}^2 + f_{air} \cdot n_{air}^2\right)^{1/2} = 1.633 \cdot d \cdot n_{eff} \quad (1)$$

where f and n_{eff} stand for the filling factor and the effective refractive index of the opal film. For a perfect fcc lattice of PS with n_{PS} ~ 1.59, one can assume $f_{PS} = 0.74$ and n_{eff} will approximately be 1.46. In Fig. 3(a), the typical reflectance spectra from five PS240

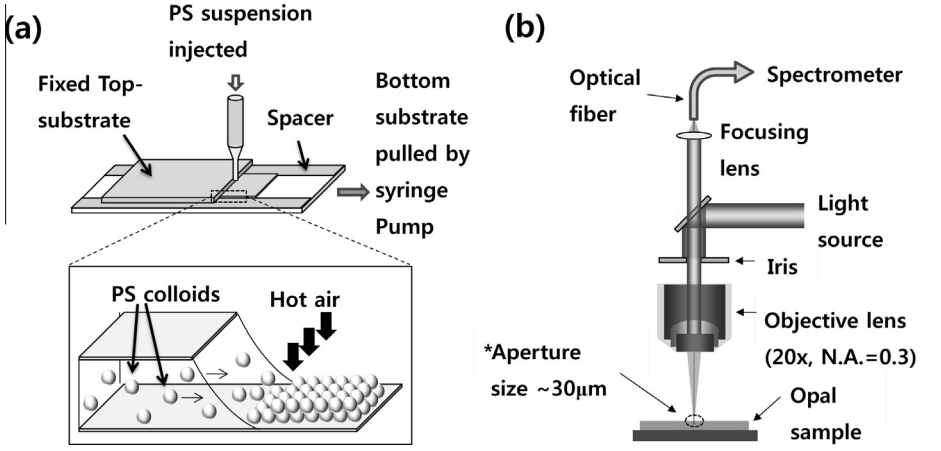

Fig. 1. Schematic illustration of (a) slide coating of PS dispersion and (b) reflectance measurement by UV–Vis spectrometer coupled with optical microscope.

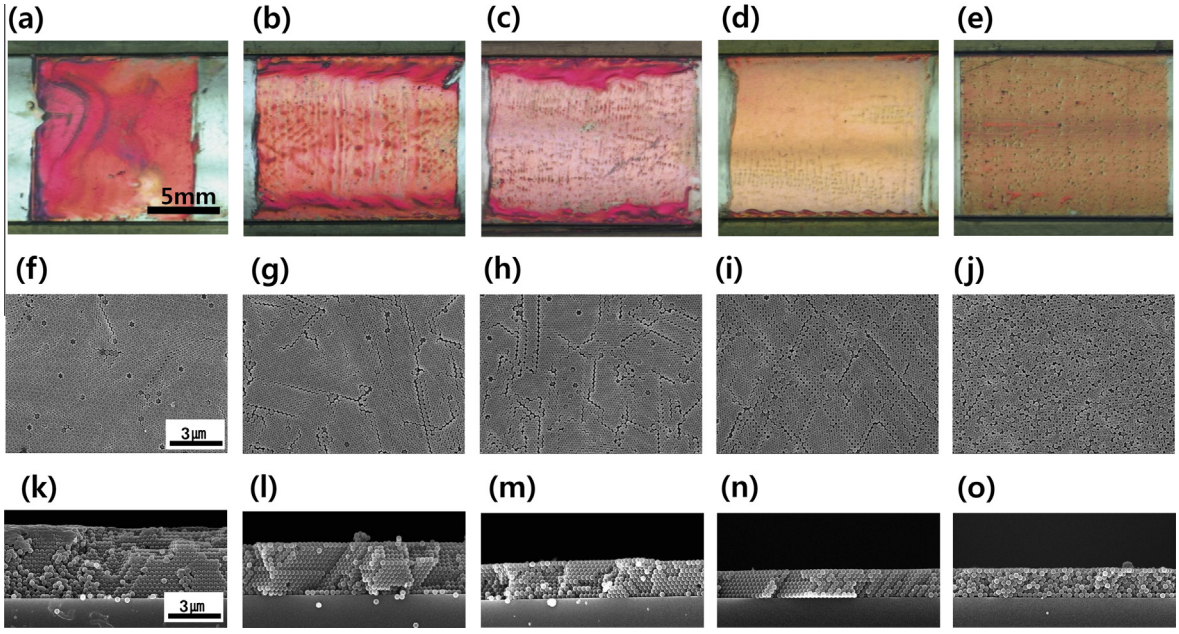

Fig. 2. (a)–(e) Optical photographs, (f)–(j) SEM top-view, and (k)–(o) SEM cross-view of PS280 opal film with varying IPA contents (25%, 40%, 50%, 60% and 75% from left).

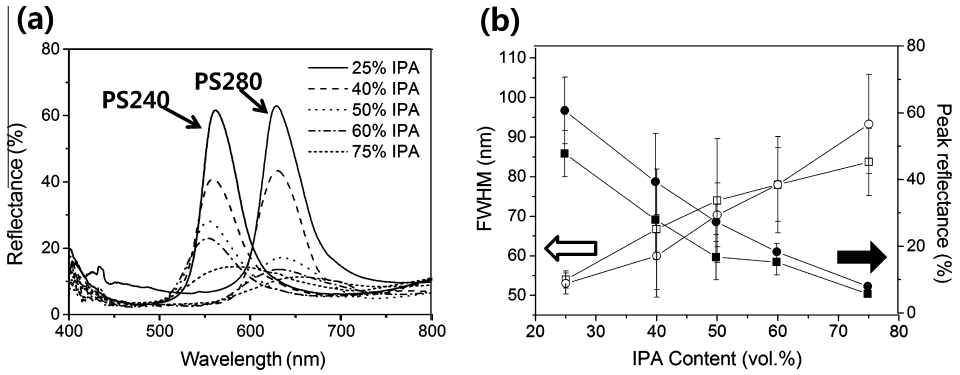

Fig. 3. (a) Reflectance spectra of opal films and (b) plots of width and peak reflectance from each peak of (a) with increasing IPA contents.

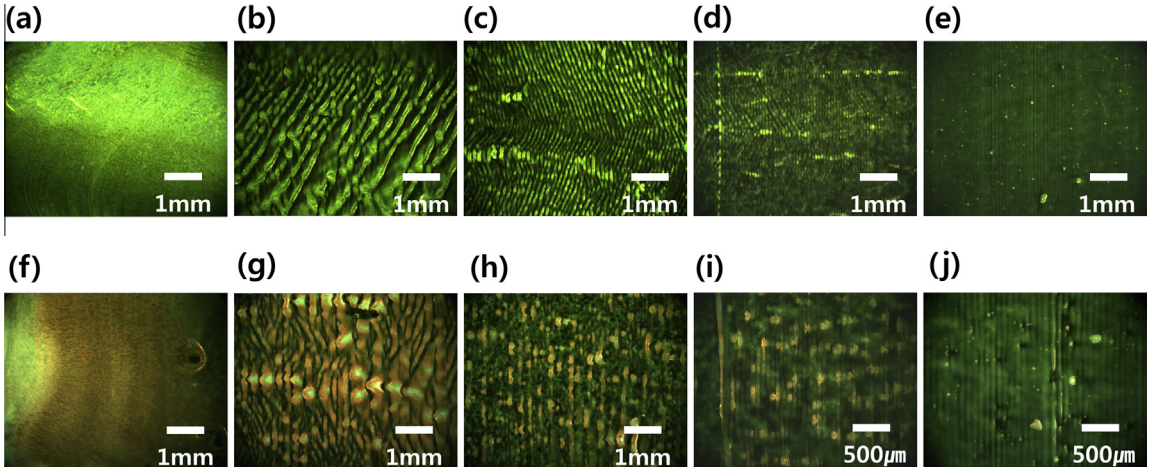

Fig. 4. Magnified optical images of the opal films fabricated from PS240 (a)–(e), and PS280 (f)–(j) at various IPA contents (a), (f) 25%, (b), (g) 40%, (c), (h) 50%, (d), (i) 60%, and (e), (j) 75%. Each film was coated from right to left.

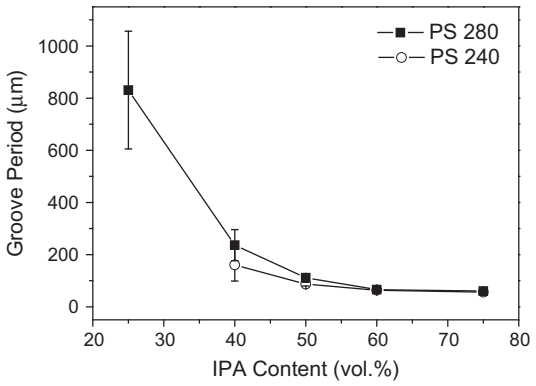

Fig. 5. Plot of groove periods in opal films with varying alcohol content in dispersing media.

films and those from PS280 films are shown, and the averaged values of the peak reflectance (λ_{peak}) and the full width at half maximum (FWHM) measured from each spectrum are plotted in Fig. 3(b). The measured λ_{peak} was in good accordance with the estimation by Eq. (1), in spite of slightly overestimated calculation results which can be attributed to smaller n_{PS} and f_{PS} in real opal film respectively due to imperfection in PS polymerization and opal packing as shown in Fig. 2. As Fig. 3(a) and (b) shows, the increased IPA content apparently caused lowering of λ_{peak} and broadening of FWHM of each reflectance peak, evidently showing the deterioration of the opal structure. In slide coating of colloidal dispersion, there are two major driving forces for the close-packed array in the opal film; (1) global movements of particles associated with a liquid flux toward drying front in equilibrium with evaporation rate, (2) capillary force exerted by the liquid meniscus between particles in the course of liquid evaporation [19]. The capillary force is directly proportional to the surface tension (γ) of the drying solvent. As IPA content increases, the surface tension of the liquid medium is lowered since the surface tension of water (γ_{water} = 72.8) is greater than that of IPA. (γ_{IPA} = 28.0) at ambient temperature [20]. Therefore, a lowering of packing density can be expected at high IPA content at the given coating conditions. In addition to the effect of reduced surface tension by increased IPA content, dilution of the colloidal suspension also affects the film reflectance. However, the colloidal suspensions diluted by water at the same concentrations did not show a notable peak broadening in the reflectance spectra (Fig. S3).

A closer look at the optical images in Fig. 2(a)–(e) reveals that the coated films on glass slides have parallel groove patterns which are aligned normal to a coating direction with varying groove periods, just like those on a diffraction grating. Such wavy film structures constantly occurred for both PS240 and PS280. Shown in Fig. 4 are the magnified optical images of the films with groove patterns which mostly appear uniformly parallel to each other, while comb-like alignments are occasionally found. With increased IPA contents, the groove periods were in decreasing tendency as shown in Fig. 5 where the averaged groove periods are plotted as a function of IPA content in the binary dispersing media. It appears that PS240 exhibits smaller periods for the given IPA content. For the PS240 film from 25% IPA dispersion, there was no observable groove-like structure.

Using a PS240 opal film from 50% IPA suspension, the groove patterns were more rigorously analyzed. As shown in Fig. 6(a)–(c), the sequentially enlarged photographic images were taken at a center region of the film from which the hierarchical structures of the groove patterns are shown. When an edge of the uphill mound is viewed by SEM, it appears to have the terraced structure of 2-dimensionally (2-D) packed colloidal arrays resembling the terraced paddy fields (Fig. 6(d)). Although a majority of the colloidal arrangements in 2-D layers showed hexagonal close-packed structures, loosely packed arrays were occasionally observed especially near the edge of the terrace. (More images of the hierarchical groove structure are shown in Fig. S4.)

In Fig. 6(e), the SEM cross-section images of a PS240 opal film taken at various spots are shown. Owing to the terraced structure of each groove, the film thicknesses vary from 0.5 to 4 μm where

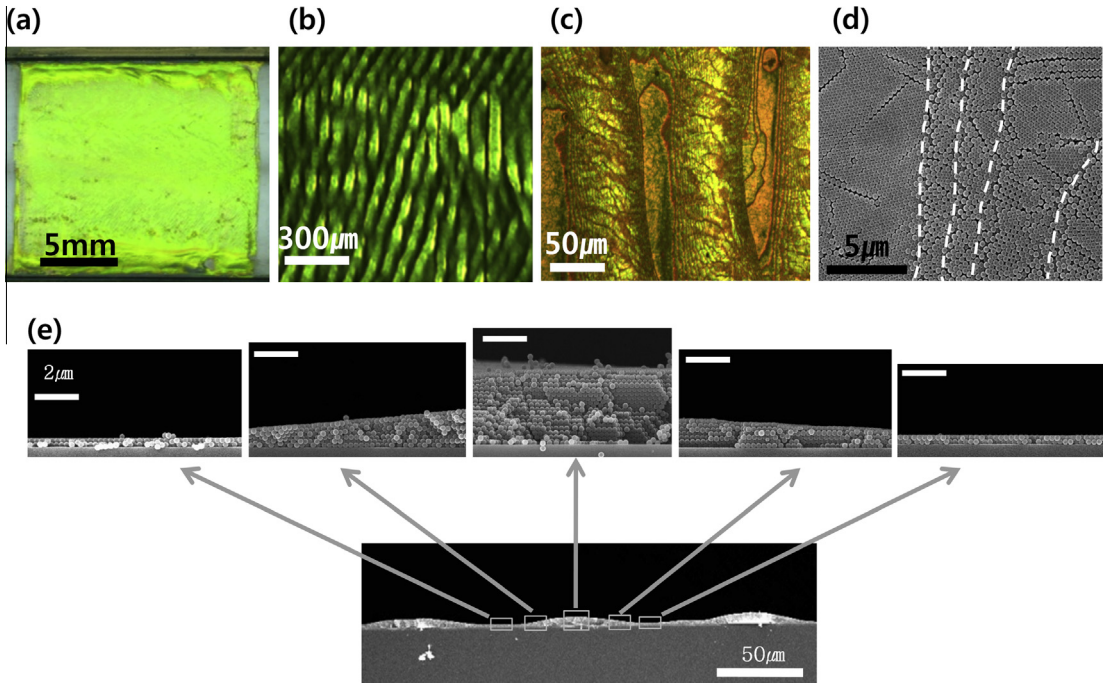

Fig. 6. (a)–(c) Optical microscopic images, and (d), (e) SEM images of slide coated opal films from PS240 dispersed in water/IPA (50/50) mixed medium. Figures are arranged in order of increasing magnification. Hierarchical structures of parallel groove patterns are evidently shown. In (d), dashed lines indicate the terraces of colloidal layers. The images shown in (e) are the cross-section SEM images at various positions.

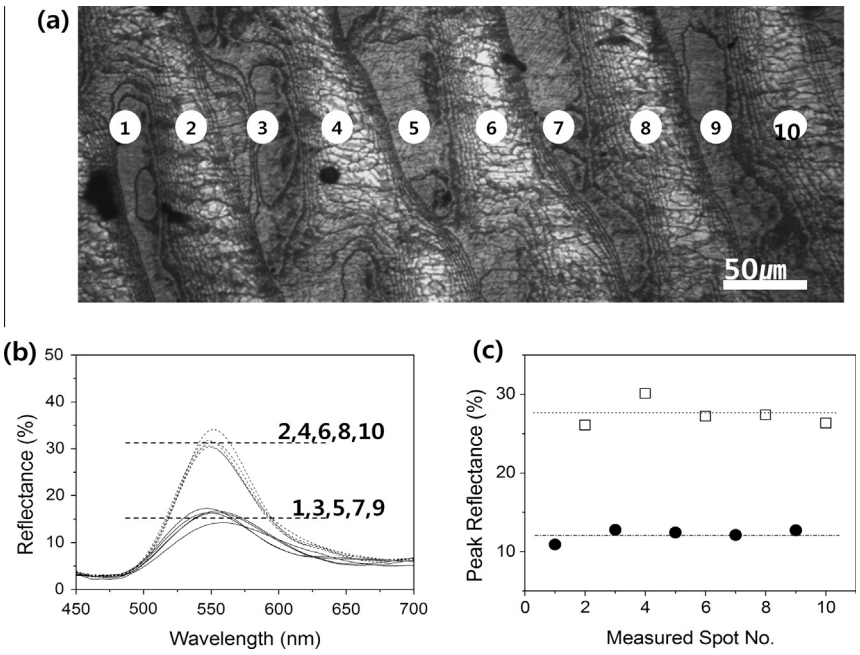

Fig. 7. (a) A magnified optical microscope image of the groove-patterned opal film. At each numbered position, reflectance spectrum was obtained with the aperture size of 30 μm which is the smallest size at the given measurement system. (b) The reflectance spectra measured at each position. From the odd numbered spots at the grooves, weak reflectances were obtained because the film thicknesses are thinner than those of even numbered spots at the peaks. (c) Alternating tendencies of the peak reflectances at odd/even numbered regions are shown.

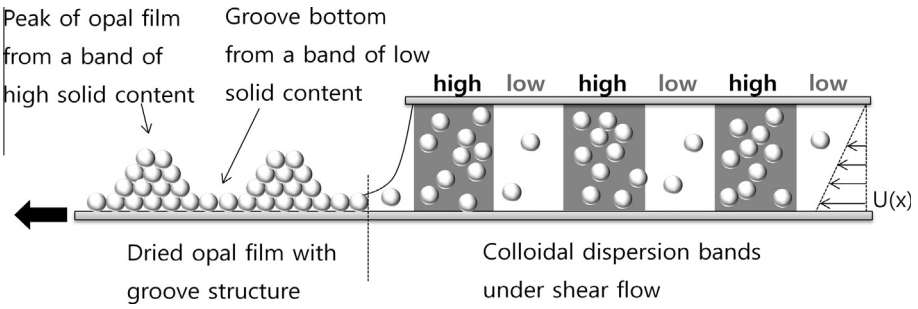

Fig. 8. Simplified schematic description of groove-like opal film formation from the oscillatory concentration bands of colloidal dispersions between two plates under shear flow.

the thinnest spot on a groove only consists of two layers of hexagonal packing structure. Since the Bragg diffraction of light originates from the interferences of the reflected light from multiple layers of alternating refractive indices, the reflective color at a groove valley will be weaker than that at a peak due to an insufficient light diffraction. In Fig. 6(b), one can easily distinguish that the darker stripes are the valleys with lower diffraction of light. In the reflectance measurement system used in this study, the smallest aperture size was 30 μm at which the diffracted light from a small circular area can be collected. With the minimum aperture size, reflectance spectra were obtained from the ten spots of PS240 opal film as indicated in Fig. 7(a), where the odd numbered spots correspond to the groove valleys and the even numbered spots are the peaks.

The measured reflectance spectra are overlaid in Fig. 7(b), and the peak reflectance values are summarized in Fig. 7(c) in which the odd numbered spots show only 50% of peak reflectances compared to those at the even numbered spots owing to the weak diffraction of the corresponding wavelength of light. Due to the finite aperture size for the reflectance measurement through which mixed light information can be collected, the reflectance data in Fig. 7(b) and (c) might actually be compensated for both odd and even numbered spots.

Generation of unique groove-patterned opal film is worthwhile to note from both academic and practical points of view. Although the origin of the topological grating-like patterns on the slide-coated opal film is not clearly understood at this stage, a possible formation of the rheologically driven oscillating bands of different particle concentrations can be suggested under a shear flow within a thin channel as schematically depicted in Fig. 8. Wang and Tong reported on the hydrodynamic instability of granular materials in rapid shear flow based on continuum rheological model where they found that the rapidly sheared particles tend to form the alternating bands or clusters of high and low solid concentrations [21,22]. Since the pulling speed of the substrate in our method is several orders of magnitude faster than that of conventional dip coating techniques [9,23], a substantial shear force is exerted to the particle dispersion between two plates during the slide coating. With the substrate pulled out, the maximum shear flow occurs at the bottom of thin channel, where a shear flow rate $U(x)$ is the

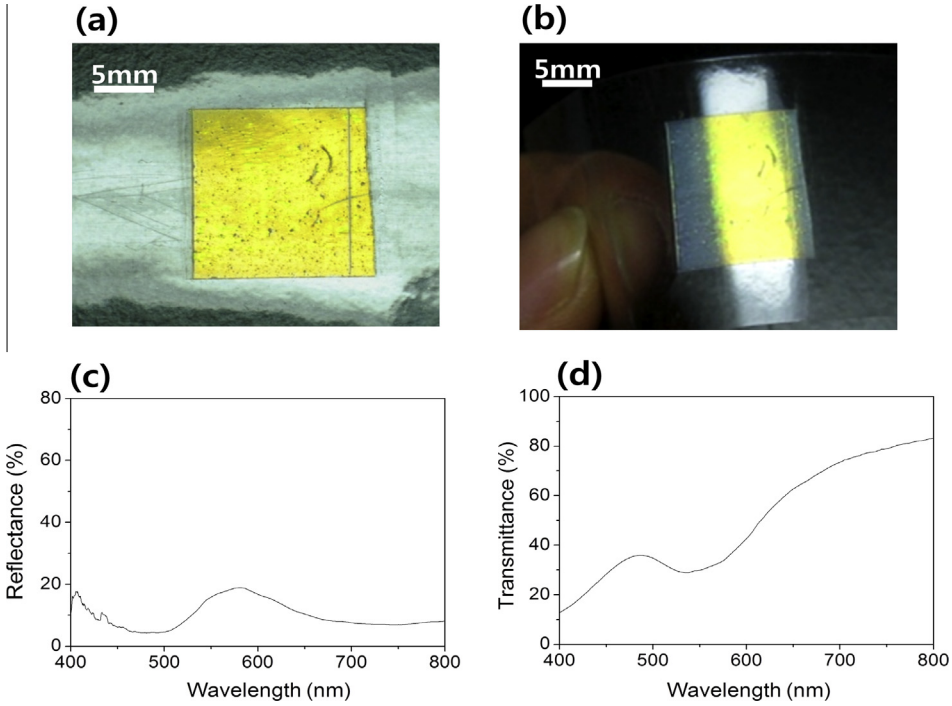

Fig. 9. (a) Optical image of a slide-coated opal film from PS240 on flexible Mylar film, (b) opal film with substrate bending, (c) reflectance spectrum and (d) transmittance spectrum of the above film showing broad stopbands appearing at the similar wavelength (~590 nm) in both spectra.

same as the substrate's pulling speed as described in Fig. 8. Once the alternating concentration bands of PS dispersion are formed inside the channel, the air-exposed dispersion will undergo evaporation-induced self assembly in which the film thicknesses are determined by colloidal concentrations of the bands as described in Fig. 8.

The experimental variables to determine the average film thickness in slide coating process are manifold such as a concentration of colloidal dispersion, channel height, and pulling speed of a substrate [8,15]. Owing to a rapid evaporation of water/IPA mixture, the concentration bands in the dispersion are believed to be directly transformed to the topological groove pattern on the film upon air exposure before redistribution of the particles by diffusion. Through *in-situ* monitoring of a slide coating, it was confirmed that the groove pattern was immediately formed as soon as the colloidal dispersion is exposed to air, and become fixed upon rapid drying of the liquid (see the video still). For comparison, the slide coating of the same colloidal particles dispersed in water was examined at the same solid contents and the same coating speed, but the topological groove patterns were not observed from any of resulting films. The coated films, however, exhibited very intense reflective colors and the reflectivities which are the evidences for the high quality opal film formation. Assuming that the suggested mechanism can be applied to the aqueous dispersion as well, the shear-driven oscillating bands of colloidal suspension which have occurred within the channel would undergo a diffusive relaxation of the concentration bands in aqueous system upon air exposure. In slide coating method, the wet colloidal film usually spends several tens of second before complete drying of water, while the alcohol dispersant has much more rapid evaporation rate to hamper the concentration relaxation.

As experimentally verified in Figs. 4 and 5, the periodic distance of the groove patterns is in decreasing order with increasing IPA content and smaller particle size. Based on the assumption that the groovy opal film originates from the oscillating bands of colloidal concentration in shear flow, the groove periods appear to be related to the viscosity of dispersing medium. In a sheared fluidic system, it has been reported that the wavelength of wave-like instability is inversely proportional to the phase velocity, which is in turn related to the particle diffusivity in the given medium [24]. The particle's diffusivity is inversely proportional to the liquid viscosity as Stoke–Einstein equation predicts. Since the liquid viscosity drops with increased IPA content in the mixed solvent, the groove periods are expected to increase with a liquid viscosity. It was confirmed that the decreasing tendency of groove period vs. IPA content is in a good accordance with that of the liquid viscosity vs. IPA content in water/alcohol mixture [25]. Rigorous interpretation of the groove period may require deeper understanding of nonlinear fluid dynamics and more experimental investigation, which are beyond the scope of this study.

Since the groove patterns are uniformly generated over entire film surface, it is expected that the patterned opal film can be efficiently utilized as a diffraction grating for the light of the wavelength range corresponding to the pitch size. Considering that the groove periods obtained in this study range in 50–500 μm, the film can be used for the optical dispersive element of IR light. In spite of the existence of micron-sized groove patterns and significant stacking faults, the PS colloidal crystals in the slide-coated opal films still show the long range orders good enough to generate Bragg diffraction of light to exhibit the shiny reflective color. Since the alcoholic medium is less hydrophilic than pure water, the colloidal dispersion in water/alcohol media can be coated on a plastic substrate which is less polar than glass slide without delamination problem. For an example, a dispersion of PS240 in water/IPA (25/75) was slide-coated on a flexible Mylar® film which had been precleaned with IPA. As shown in Fig. 9(a), a reflective opal film was obtained on Mylar film without dewetting problem. After being annealed in vacuum oven at 90 °C for 24 h, the opal film showed better adhesion with a flexible substrate, and the film quality was not affected by bending of Mylar film (Fig. 9(b)).

As shown in Fig. 9(c) and (d), it was confirmed that the stopband positions and their bandwidths of an opal film were almost

the same in both reflectance and transmission spectra, implying that the colloidal packing structures were maintained throughout whole thickness range. Opal films on flexible substrate are expected to find wider variety of applications, and therefore the rigorous investigations on the effect of various substrates on slide coating will be followed soon.

4. Conclusions

Spherical PS dispersions in water/IPA binary liquid were coated on glass substrates via slide coating method which is capable of rapid fabrication of opal films. The coated opal film became more defective with the increased IPA content due to a reduction of capillary force that hampers close packing of the colloidal particles. The coated film exhibited unique topological groove patterns with decreasing groove period upon dilution with IPA. The groove pattern is expected to be originated by a periodic instability of colloidal concentration within the channel under strong shear force exerted during the slide coating process. The groove periods were observed to be proportional to the solvent viscosity which decreases with increasing IPA content. Colloidal particle size also affected the groove period presumably owing to the different particle diffusivities in viscous media. Topological groove patterns are as uniform as it can be utilized as the diffraction grating for IR light based on their pitch sizes. Due to a lowered hydrophilicity in water/IPA dispersant, the slide coating of opal film could be successfully carried out on a flexible Mylar film without significant dewetting problem.

Acknowledgments

This study was supported by the Basic Science Research Program through the National Research Foundation of Korea (NRF) funded by the Ministry of Education, Science and Technology (2012R1A1A2021880), and partially supported by the Basic Science Research Program through the National Research Foundation of Korea (NRF) funded by the Ministry of Education, Science and Technology, Korea (2013R1A1A2011168).

Appendix A. Supplementary data

Supplementary data associated with this article can be found, in the online version, at http://dx.doi.org/10.1016/j.jcis.2014.10.051.

References

[1] S.V. Frolov, Z.V. Vardeny, A.A. Zakhidov, R.H. Baughman, Opt. Comm. 162 (1999) 241.
[2] O. Painter, R.K. Lee, A. Scherer, A. Yariv, J.D. O'Brien, P.D. Dapkus, I. Kim, Science 284 (1999) 1819.
[3] K. Lee, S.A. Asher, J. Am. Chem. Soc. 122 (2000) 9534.
[4] Y.J. Lee, P.V. Braun, Adv. Mater. 15 (2003) 563.
[5] B. Griesebock, M. Egen, R. Zentel, Chem. Mater. 14 (2002) 4023.
[6] M.H. Kim, S.H. Im, O.O. Park, Adv. Funct. Mater. 15 (2005) 1329.
[7] J.H. Zhang, Z.Q. Sun, B. Yang, Curr. Opin. Colloid Interface Sci. 14 (2009) 103.
[8] S.H. Im, M.H. Kim, O.O. Park, Chem. Mater. 15 (2003) 1797.
[9] Y.A. Vlasov, X.Z. Bo, J.C. Sturm, D.J. Norris, Nature 414 (2001) 289.
[10] A. Mihi, M. Ocana, H. Miguez, Adv. Mater. 18 (2006) 2244.
[11] Y.N. Jiang, H. Li, X.S. Meng, D.F. Zhao, Y.Y. Wang, Q. Liu, J. Zheng, J.H. Zhang, Q. Lin, B. Yang, J. Rare Earths 26 (2008) 932.
[12] H.L. Li, W.T. Dong, H.J. Bongard, F. Marlow, J. Phys. Chem. B 109 (2005) 9939.
[13] W. Lee, A. Chan, M.A. Bevan, J.A. Lewis, P.V. Braun, Langmuir 20 (2004) 5262.
[14] H.T. Yang, P. Jiang, Langmuir 26 (2010) 13173.
[15] S.C. Gil, Y.G. Seo, S. Kim, J. Shin, W. Lee, Thin Solid Films 518 (2010) 5731.
[16] Y.G. Seo, J. Woo, H. Lee, W. Lee, Adv. Funct. Mater. 21 (2011) 3094.
[17] S. Kim, Y.G. Seo, Y. Cho, J. Shin, S.C. Gil, W. Lee, Bull. Kor. Chem. Soc. 31 (2010) 1891.
[18] H.L. Li, F. Marlow, Chem. Mater. 18 (2006) 1803.
[19] A.S. Dimitrov, K. Nagayama, Langmuir 12 (1996) 1303.
[20] G. Vazquez, E. Alvarez, J.M. Navaza, J. Chem. Eng. Data 40 (1995) 611.
[21] C.H. Wang, Z. Tong, J. Fluid Mech. 435 (2001) 217.
[22] C.H. Wang, Z. Tong, Chem. Eng. Sci. 435 (1998) 217.
[23] P. Jiang, J.F. Bertone, V.L. Colvin, Science 291 (2001) 453.
[24] E.D.M. Franklin, J. Braz. Soc. Mech. Sci. Eng. 32 (2010) 460.
[25] Y. Tanaka, Y. Matsuda, H. Fujiwara, H. Kubota, T. Makita, Int. J. Thermophys. 8 (1987) 147.